ACS APPLIED POLYMER MATERIALS

pubs.acs.org/acsapm Article

Deep Learning Analysis of the Propagation of Stabilizing Additive Hydrolysis in a Cross-Linked Polyethylene Pipe

Joseph D'Amico, Michael Grossutti, and John R. Dutcher*

Cite This: https://doi.org/10.1021/acsapm.3c02209 Read Online

ACCESS | Metrics & More | Article Recommendations

ABSTRACT: Cross-linked polyethylene (PEX-a) pipe is being increasingly used for water transport and heating applications. Its long-term stability is improved through the addition of stabilizing additive molecules that protect the pipe from environmental factors such as exposure to hot water, chlorine, and UV light. We have used infrared (IR) microscopy to measure line profiles of IR spectra across the pipe wall thickness for pipes that have been exposed to recirculating hot water at different fixed temperatures T for different aging times t. To analyze this large body of data, we used a deep learning approach involving a β-variational autoencoder (β-VAE) model. The leading latent variable L1 corresponds to the hydrolysis of a stabilizing additive molecule, and we track the penetration depth δ of the hydrolysis front radially outward from the inner wall of the pipes. The radial profiles of L1 collected for different aging temperatures T and times t allow us to interpret the propagation of the hydrolysis front as a simple diffusion process for which the activation energy E_a is large compared with the thermal energy k_BT. In addition, we determine time scaling factors $a(T)$ for the data sets collected at different temperatures T that allow us to collapse all of the data onto a master curve of δ versus scaled aging time $t' = a(T)t$, and to determine that an increase in the aging temperature T of 10 °C corresponds to a decrease in the aging time t by a factor of 1.8. Our results illustrate a distinct advantage of the β-VAE analysis: it provides a useful, interpretable representation of our very large data set, allowing us to achieve a detailed physical understanding of the stabilizing additive hydrolysis phenomenon.

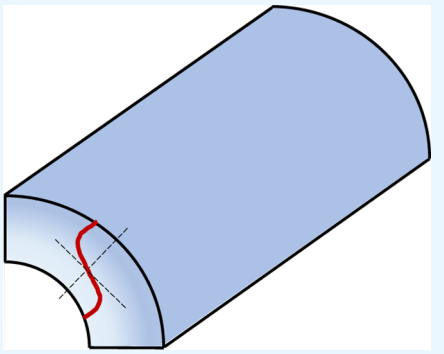

KEYWORDS: *accelerated aging, hydrolysis of stabilizing additives, cross-linked polyethylene pipe, β-variational autoencoders, diffusion, time−temperature superposition*

INTRODUCTION

Cross-linked polyethylene (PEX-a) pipe is increasingly being used to replace metal piping for domestic and industrial water transport and heating applications driven by cost savings and ease of installation. To improve the in-service lifetime of PEX-a pipe, stabilizing additive molecules are incorporated to improve the resistance of the pipes to effects such as oxidation and exposure to UV light.[1,2] For example, hindered amine light stabilizer (HALS) molecules such as Chimassorb 944 and Tinuvin 622 are often formulated as oligomers of the basic functional unit;[3,4] oligomerization increases their size and molecular weight, immobilizing them within the polymer matrix and reducing their volatility. However, during in-service use, stabilizing additives can undergo hydrolysis and photodegradation, which can lead to a reduction in the molecular weight and increased mobility within the polymer matrix.[5−9]

To mimic and exaggerate the effects of in-service use and to evaluate the long-term reliability of PEX-a pipe, accelerated aging studies have been performed by exposing the pipes to water under various conditions, e.g., elevated temperature, pressure, and degree of chlorination.[6,10−14] Previously, we used infrared (IR) microscopy to compare the accelerated aging of PEX-a pipe at a fixed elevated temperature of 85 °C in either hot air or hot water.[2] In this study, the IR spectra were averaged over the central portion of the radial extent of the pipe wall to avoid contributions and the associated complexity from the inner and outer pipe surfaces, and we used a principal component analysis (PCA) to determine the leading principal components responsible for the variance in the data and to track their evolution with aging time. For exposure to hot water, this allowed us to determine a surprisingly short time scale τ of 2.7 days for the hydrolysis of a stabilizing additive.[2]

One of the challenging aspects of using IR microscopy to study the spatial distribution of IR spectra of different samples aged under different environmental conditions is understanding the large amount of data that is generated. Instead of using a univariate analysis to focus on specific IR absorption

Received: September 16, 2023
Revised: November 21, 2023
Accepted: November 22, 2023

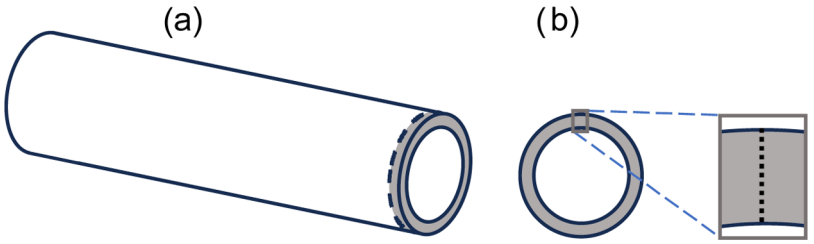

Figure 1. (a) Schematic diagram of a side view of a PEX-a pipe. An axial slice that is removed from the end of the pipe using a microtome is shown in gray. (b) Schematic diagram of an axial slice of the PEX-a pipe. The dashed line in the expanded view indicates the radial direction along which IR spectra are collected to obtain a radial profile.

bands to interpret these large amounts of data as has been done in previous studies,[9,15−18] machine learning approaches such as deep or generative learning have been used recently in the field of materials science to provide new insights into the analysis of large amounts of spectroscopy and microscopy data.[19−21] Recently, we developed a deep learning β-variational autoencoder (β-VAE) model to analyze IR spectra of PEX-a pipe.[22,23] β-VAEs are a class of deep generative models that can learn disentangled (independent and interpretable) representations of the generative factors responsible for variance in data.[24−26] We previously trained our β-VAE model on a diverse data set of 25,000 IR spectra of PEX-a pipe exposed to different environmental conditions.[22] We learned three informative latent dimensions corresponding to three physicochemical processes responsible for the variance in the IR microscopy data: the most informative latent dimension, L1, which describes the hydrolysis of a stabilizing additive; the second latent dimension, L2, which describes the oxidative degradation of amorphous polyethylene; and the third latent dimension, L3, which describes crack-specific degradation characterized by ketone carbonyl and conjugated alkene formation. We have recently applied a pretrained β-VAE model to hyperspectral IR images of PEX-a pipe,[23] which yielded high lateral spatial resolution maps of physicochemical changes to the pipe samples (latent variables L1, L2, and L3) produced by aging. This capability allowed us to characterize localized changes in the latent variables, e.g., line profiles of the stabilizing additive hydrolysis associated with L1 and the presence of cracks in the pipes associated with L3.

In the present study, we build on the success of our recent work[22,23] to apply our pretrained β-VAE model to line profiles of IR spectra measured across the wall thickness of PEX-a pipes that have been exposed to recirculating water at different fixed temperatures T for different aging times t. Exposure of the inner surface of the pipes to hot water causes hydrolysis of the ester linkages within the oligomeric stabilizing additive,[2] and this leads to the propagation of the hydrolysis of a stabilizing additive from the inner pipe surface. Specifically, we track the L1 latent variable, which is due to the hydrolysis of the stabilizing additive,[22,23] with aging time t at different fixed aging temperatures T. By fitting the radial profiles of L1 to a sigmoidal function of the radial distance r, we interpret the propagation of the penetration depth δ of the hydrolysis as a simple one-dimensional diffusion process, which allows the determination of the activation energy for the diffusion process. This analysis also allows us to determine that an increase in aging temperature of 10 °C produces a degree of hydrolysis that is equivalent to a decrease in the aging time by a factor of 1.8. The results of the present study demonstrate that a deep learning approach offers considerable promise to process and interpret a large amount of spectroscopic data in terms of simple physical models.

MATERIALS AND METHODS

Sample Preparation and Accelerated Aging of PEX-a Pipe. For the accelerated aging experiments, we used segments of PEX-a pipes (HeatLink; 12.7 mm inner diameter, 2.0 mm wall thickness, approximately 6 cm in length). We exposed these pipe segments to recirculating distilled water held at four different fixed temperatures T—60, 70, 80, and 90 °C—for aging times t ranging from 3 days to 90 days. At different time points during the aging experiments, we removed the pipes from the recirculating water setup and used an American Optical model 820 rotary microtome to obtain thin slices of the pipe perpendicular to the extrusion direction (axial slices; Figure 1).[2] To avoid the pipe sample ends, where the pipe was coupled to fittings on the recirculating water system, we used the microtome to remove thick slices from the ends of the pipe samples until the combined thickness of the removed slices was ∼4 mm (>pipe wall thickness). The microtome was then used to produce thin (∼200 μm thick) axial slices that were used in the FTIR microscopy experiments.

Infrared Microscopy Measurements. We measured transmission IR absorption spectra on axial slices using a Thermo/Nicolet Continuum Infrared Microscope equipped with an MCT detector at a resolution of 4 cm^{-1}. Approximately 30 spectra were collected, in 100 μm increments, across the wall thickness of each axial slice to obtain a radial profile of each sample, as shown schematically in Figure 1b.[2] Each spectrum represents the average IR absorption over a 50 × 50 μm area (at a given radial depth r), expressed in absorbance units

$$A = -\log(I/I_0) \quad (1)$$

where I and I_0 are the single beam intensities transmitted through the pipe slice and air, respectively.

Spectra Preprocessing. IR spectra were preprocessed in Quasar[27] by baseline correcting the spectra and normalizing the absorbance values by the 2019 cm^{-1} band, which arises from both amorphous and crystalline regions of polyethylene, to correct for variations in sample thickness.[2] The frequency regions selected for analysis were 1800−1520 and 1200−895 cm^{-1}. These frequencies correspond to the fingerprint region of the IR spectra, excluding strong and saturated absorptions from the polyethylene.

β-Variational Autoencoder (β-VAE) Model Training and Hyperparameters. To analyze the dependence of the IR spectral features on aging time and temperature, we applied a pretrained neural network β-variational autoencoder (β-VAE) to identify and quantify the generative factors of variance in our spectroscopic data set. A detailed description and derivation of the β-VAE framework is described in detail in refs 24−26, and the coded implementations are provided in refs 28−30. Briefly, the β-VAE model consists of an encoder neural network, which encodes the input as random variables with a Gaussian probability distribution, and a decoder neural network, which samples latent values obtained from the probability distribution. The β-VAE loss function minimized by the neural network optimizer is the sum of two components: the mean squared error (MSE) of the reconstruction compared to the input and a scaled

https://doi.org/10.1021/acsapm.3c02209
ACS Appl. Polym. Mater. XXXX, XXX, XXX−XXX

Kullback–Leibler (KL) divergence term, where the KL divergence measures the difference between two probability distributions[24−26]

$$\beta\_\mathrm{VAE}_{\mathrm{loss}} = \mathrm{MSE}_{\mathrm{loss}} + \beta \cdot \mathrm{KL}_{\mathrm{divergence}} \quad (2)$$

Typically, $\beta > 1$, which increases the weight of the $\mathrm{KL}_{\mathrm{divergence}}$ term in the loss function relative to that of the $\mathrm{MSE}_{\mathrm{loss}}$ term.[24,25] The balance between the two terms in eq 2 is tuned by the choice of β. The most informative learned latent dimensions are identified as those with the largest $\mathrm{KL}_{\mathrm{divergence}}$ cost that produce the largest changes in the decoded spectra while holding the other latent dimensions constant.[23]

The β-VAE model was implemented in Python with TensorFlow[31] and Keras.[32] The input layer was 300 units, corresponding to an IR spectrum consisting of 300 data points. The encoder consisted of two fully connected 128-unit layers with ReLu activations. The latent dimension consisted of 8 units (8 units mean and 8 units standard deviation layer). The decoder consisted of two fully connected 128-unit layers with ReLu activations and a 300-unit output layer corresponding to the reconstructed IR spectrum, with linear activations. The model was trained on a data set of ~25,000 IR spectra of virgin, in-service, cracked, and aged PEX-a pipe using an Adam optimizer[33] with a learning rate of 10^{-4} and $\beta = 7$.

RESULTS AND DISCUSSION

The recirculating water aging experiments produced systematic changes to the IR spectra of the PEX-a pipe samples with aging at a fixed temperature T for different aging times t. Representative changes in the IR spectra are illustrated in Figure 2a, in which we highlight the spectral ranges containing the vibrations corresponding to the ester C═O (carbonyl) and C−O bonds collected on a PEX-a pipe exposed to recirculating water at T = 80 °C for different aging times t. The arrows indicate the direction of changes in the IR peak absorbances with increasing aging time t. Specifically, with increasing t, we observed decreases in the absorbance of the ester C═O and C−O peaks, centered at 1740 and 1170 cm^{-1}, respectively, as well as increases in the absorbance of the COOH and COO^- peaks, centered at 1700 and 1570 cm^{-1}, respectively. These changes are consistent with hot water-driven hydrolysis of stabilizing additive ester linkages, as observed in previous studies.[2,22,23,34−39]

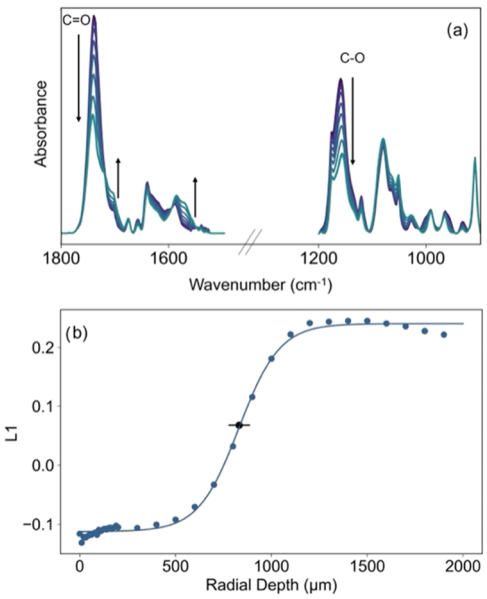

Figure 2. (a) IR absorbance versus wavenumber at a fixed radial position r for a PEX-a pipe exposed to recirculating water at 80 °C for different aging times t ranging from 0 to 42 days, shown with different colors, highlighting the spectral ranges containing the vibrations corresponding to the ester C═O (carbonyl) and C−O bonds. The direction of the arrows corresponds to increasing values of t. (b) Representative plot of the average value of the L1 latent parameter versus radial depth r (blue symbols) for a PEX-a pipe exposed to recirculating water at 80 °C for 21 days. The inner surface of the pipe corresponds to r = 0. The solid curve corresponds to the best fit of the data to the sigmoidal equation specified by eq 3, characterized by the penetration depth δ at the midpoint, as indicated by the solid black circle with a short horizontal black line, of the sigmoidal function of width Δ.

In the β-VAE analysis of the IR data, the most informative latent variable L1 describes hot water-driven hydrolysis of the stabilizing additive ester linkages.[22,23] The hot water flowing past the pipe's inner wall surface results in the hydrolysis of the stabilizing additive, which propagates outward from the inner wall with increasing aging time t. We use radial profiles of L1, such as that shown in Figure 2b, to track the penetration of the hydrolysis of the stabilizing additive through the pipe wall thickness. At large radial distances, the value of L1 is positive and large, corresponding to the stabilizing additive molecules that have not been hydrolyzed. Near the pipe's inner wall, the value of L1 is large and negative, corresponding to hydrolyzed stabilizing additive molecules. The transition between hydrolyzed and unhydrolyzed stabilizing additive molecules with increasing radial depth r can be seen clearly in Figure 2b, and it is well described by a sigmoidal function (solid curve in Figure 2b)

$$\mathrm{L1}(r) = a_0 + \left[\frac{a_1}{1 + e^{(\delta - r)/\Delta}}\right] \quad (3)$$

which allows us to quantify the midpoint of the transition (inflection point of the sigmoidal function), which we call the penetration depth δ, as well as the width of the transition Δ.

In Figure 3, we show radial profiles of L1 for different aging times t and temperatures T. For each value of T, we can see that the radial profiles penetrate through the pipe wall thickness with increasing aging time t and, with increasing aging temperature T, the penetration of the radial profiles proceeds more quickly through the pipe wall thickness. As in Figure 2b, each radial profile in Figure 3 is well described by the sigmoidal function in eq 3, and the best-fit curves for each data set are shown as solid curves in Figure 3 using the same color as the corresponding data set. We note that we obtain similar maximum and minimum values of L1 for all profiles, indicating the robust nature of the L1 values determined for the data set. We have added short horizontal black lines to most of the data sets in Figure 3 that correspond to the midpoints or inflection points of the best-fit sigmoidal functions, which we define to be the penetration depth values δ.

The radially outward propagation of the L1 radial profiles is driven by the hydrolysis of ester linkages within the stabilizing additive molecules. This leads to a decrease in the degree of polymerization of the oligomeric stabilizing additive molecules, increasing their mobility within the polyethylene matrix. The hydrolysis of ester linkages in the stabilizing additive begins near the inner pipe wall upon exposure to hot water. This creates smaller, more mobile fragments of the oligomeric additive that can diffuse within the polyethylene matrix, and the carboxylic acid products can catalyze further hydrolysis within the same and different stabilizing additive molecules, a

https://doi.org/10.1021/acsapm.3c02209
ACS Appl. Polym. Mater. XXXX, XXX, XXX−XXX

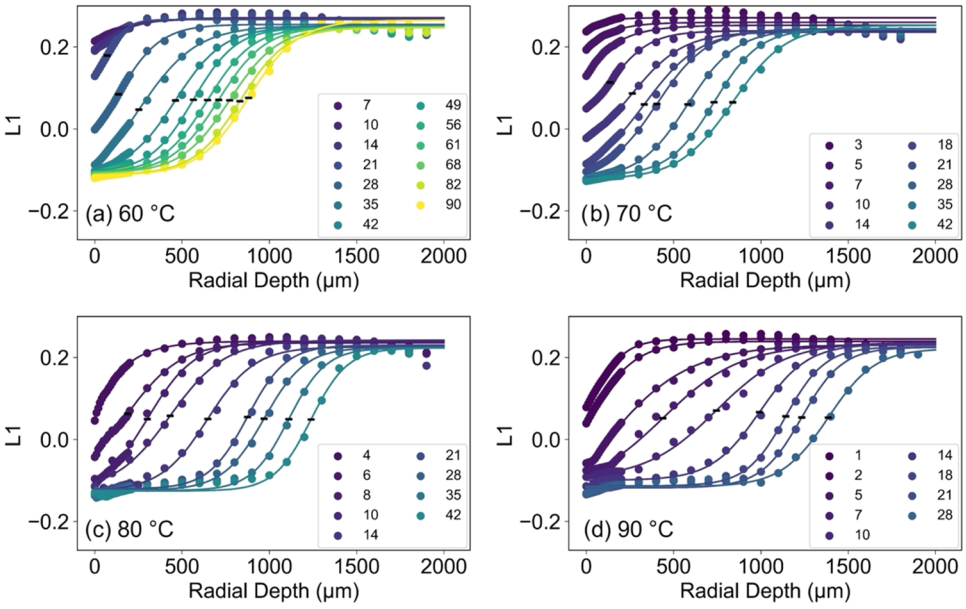

Figure 3. Average values of the L1 latent parameter versus radial depth r for PEX-a pipes exposed to recirculating water at different temperatures T: (a) 60 °C, (b) 70 °C, (c) 80 °C, and (d) 90 °C. The inner surface of the pipes corresponds to $r = 0$. In each plot, symbols with different colors correspond to different aging times t in days, as indicated in the corresponding legend, and the best-fit curve of each data set to eq 3 is shown in the same color. The midpoint of the transition (penetration depth, δ) for each best-fit curve is indicated by a short horizontal black line.

process known as autocatalysis. As a result, the diffusion of the small fragments of the stabilizing additive radially outward from the pipe's inner wall leads to the radial propagation of the hydrolysis front in a process called diffusion-limited hydrolysis,[40] which we observe as the outward propagation of the L1 radial profile with corresponding penetration depth δ.

The above interpretation suggests that the dependence of the penetration depth δ on aging time t can be described by a simple diffusion process with a $t^{1/2}$ dependence

$$\delta(t) = A(t - t_0)^{1/2} \tag{4}$$

where we have allowed for an onset time t_0 for significant diffusion to occur. For the one-dimensional diffusion of small molecules, the root-mean-square displacement x_{rms} is written as

$$x_{rms}(t) = (2Dt)^{1/2} \tag{5}$$

where D is the diffusion coefficient, so that, in our interpretation of the penetration of the hydrolysis process as a diffusion process (eq 4), $\delta(t)$ corresponds to $x_{rms}(t)$, and we interpret the coefficient A as $(2D)^{1/2}$.

In Figure 4, we plot the penetration depth δ versus aging time t for the four different aging temperatures T, together with solid curves that correspond to the best fits of eq 4 to each data set at each value of T. The agreement between the data and best-fit curves is very good, with r^2 values greater than 0.96. At each temperature T, there is a significant onset time $t_0(T)$ before the hydrolysis front moves radially outward from the inner wall of the pipe (Figure 4a), with t_0 decreasing significantly with aging temperature T (Figure 4b). The large, temperature-dependent values of t_0 are consistent with attributing the propagating hydrolysis front to the diffusion of fragments of the stabilizing additive molecules since diffusion of a small molecule like water should not experience a significant delay in its diffusion. It seems that sufficient hydrolysis of the stabilizing additive molecules has to occur before the small fragments can diffuse radially outward, catalyzing further hydrolysis at larger radial distances.

We can gain further insight into the hydrolysis process by utilizing the concept of time−temperature superposition.[41] In this approach, we determine scaling factors $a(T)$ that allow us to scale the aging times t such that the data sets collected at different temperatures T collapse onto a single master curve for a chosen reference temperature T_{ref}. This scaling analysis allows us to determine the change in aging time t corresponding to a given increase in temperature T. To determine the scaling required for the collapse of the data onto a single master curve, we can use the best-fit curves shown in Figure 4a. We choose a common value of δ, in this case, δ = 600 nm (30% of the pipe wall thickness), and solve eq 4 at each temperature T for the corresponding value of the aging time t at each of the four measurement temperatures T. To obtain the collapse of all of the data sets, we choose a reference temperature T_{ref} = 80 °C, determine the ratio $a(T) = t(T = T_{ref})/t(T)$, and calculate the scaled times $t' = a(T)t$. In Figure 5, we show the corresponding master plot of penetration depth δ versus scaled aging time t', and the overlap of the different scaled data sets is very good. Based on this analysis, the average value of the scaling factor $a(T)_{\Delta T=+10\ °C}$ corresponding to an increase in temperature by 10 °C within the 30 °C temperature measurement range is 1.8. This provides a useful rule of thumb for the penetration of the hydrolysis of the stabilizing additive: an increase in the aging temperature T of 10 °C corresponds to a decrease in the aging time t by a factor of 1.8.

We can use our measurements of the temperature dependence of the penetration depth δ to calculate the activation energy E_a associated with the diffusion process. The diffusion of small molecules is typically interpreted as an Arrhenius process for which the temperature dependence of the diffusion coefficient $D(T)$ is given by[42]

$$D(T) = D_0 \exp(-E_a/k_B T) \tag{6}$$

https://doi.org/10.1021/acsapm.3c02209
ACS Appl. Polym. Mater. XXXX, XXX, XXX−XXX

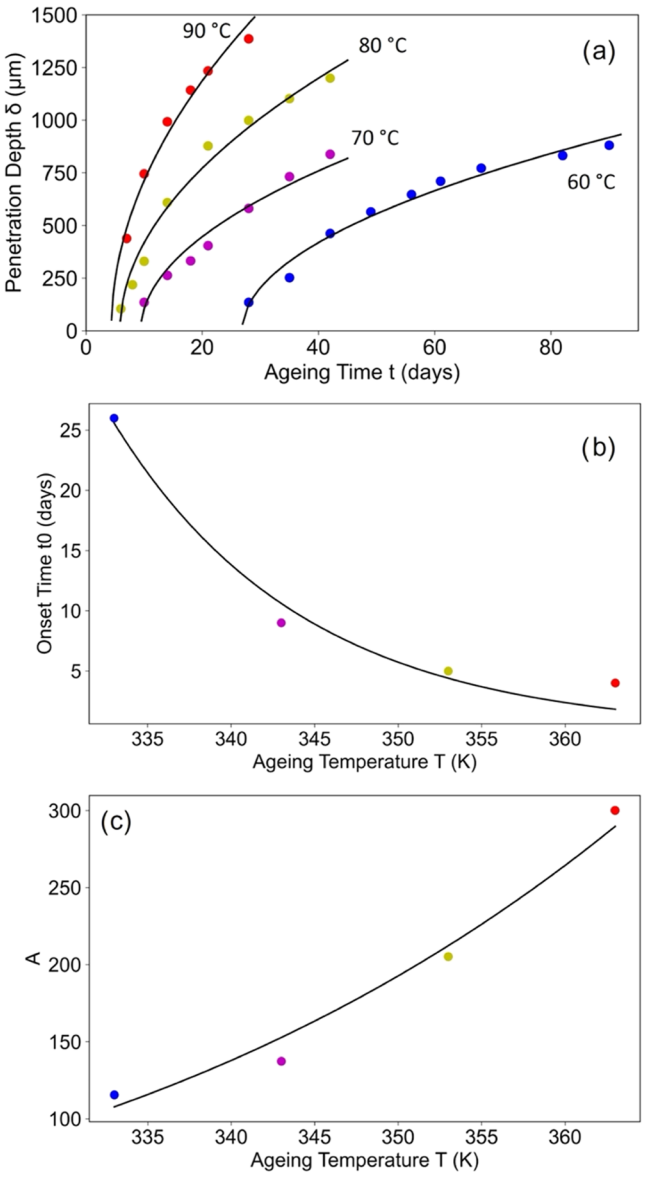

Figure 4. (a) Penetration depth δ versus aging time t for the data shown in Figure 3 for PEX-a pipes exposed to recirculating water at different temperatures (T = 60 °C (blue circles), 70 °C (purple circles), 80 °C (gold circles), and 90 °C (red circles)). The solid curves correspond to the best fits of each data set to eq 4. (b) Best-fit values of the onset time t_0 (defined in eq 4) versus aging temperature T obtained from the best fits to the data shown in Figure 4a. The solid curve corresponds to the best fit of the $t_0(T)$ data to an exponential function. (c) Best-fit values of the prefactor A (defined in eq 4) versus aging temperature T obtained from the best fits to the data shown in Figure 4a. The solid curve corresponds to the best fit of the $A(T)$ data to eq 7, in which we use the best-fit value of the activation energy E_a associated with the diffusion process, as determined below.

where D_0 is a temperature-independent coefficient, E_a is the activation energy for the diffusion process, k_B is Boltzmann's constant, and T is the absolute temperature. The best-fit values of A can be used to obtain the corresponding values of $D = A^2/2$, with the temperature dependence of A given by

$$A(T) \sim \exp\left(-E_a/(2k_BT)\right) \tag{7}$$

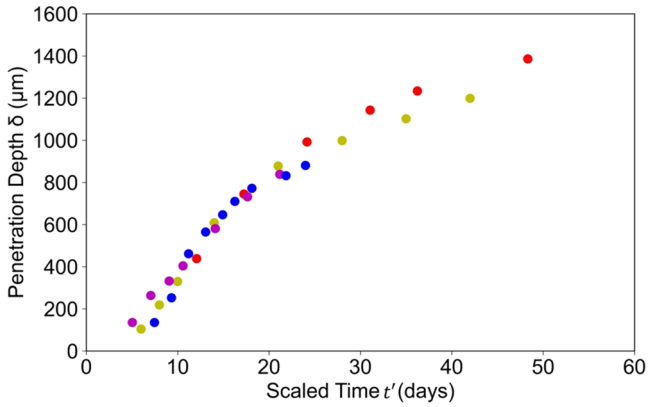

Figure 5. Master plot of penetration depth δ versus scaled aging time $t' = a(T)t$ for the data shown in Figure 4a for PEX-a pipes exposed to recirculating water at different temperatures (T = 60 °C (blue circles), 70 °C (purple circles), 80 °C (gold circles), and 90 °C (red circles)). The scaling factors $a(T)$ have been calculated so that all of the data sets overlap with that measured at the reference temperature T_{ref} = 80 °C.

The values of D can be compared at the highest and lowest measurement temperatures to obtain an expression for the activation energy E_a

$$E_a = \frac{-k_B \ln (D_H/D_L)}{\left(\frac{1}{T_H} - \frac{1}{T_L}\right)} \tag{8}$$

where D_H (D_L) and T_H (T_L) correspond to the diffusion coefficient and temperature values at the highest (lowest) measurement temperature. Substituting the best-fit values of D_H = 45,000 nm^2/s, D_L = 6600 nm^2/s, T_H = 363 K, and T_L = 333 K yields a value of E_a = 1.1 × 10^{-19} J. To assess the magnitude of E_a, we can compare it to the average value of the thermal energy k_BT_{av}, where T_{av} is the average measurement temperature of T = 348 K, and we find that $E_a/(k_BT_{av})$ = 22, corresponding to a relatively high energy barrier for the hydrolysis diffusion process. Despite this rather large value of E_a, we note that the hydrolysis of the stabilizing additive molecules occurs on a time scale (of the order of tens of days) that is very short compared with the desired lifetime of PEX-a pipes (many decades). This result provides an incentive for the PEX-a pipe industry to develop stabilizing additives that provide the desired protection for a much larger fraction of the pipe's lifetime.

It is challenging to relate the results of the present study for PEX-a pipe aged by recirculating hot water to those obtained for PEX-a pipe aged by immersion in hot water in ref 2 because of differences in the nature of the exposure of the pipe surfaces to hot water: for recirculated heating, only the inner pipe surface is exposed to hot water, with the outer pipe surface exposed to room temperature air, whereas for immersion heating, both pipe surfaces are exposed to hot water. As a result, for hot water at the same elevated temperature, the time scale for hydrolysis for immersion heating,[2] propagating away from both pipe surfaces, is smaller for immersion heating than for recirculated heating, as measured in the present study.

SUMMARY AND CONCLUSIONS

We have used a pretrained β-VAE deep learning model to study the propagation of the hydrolysis of a stabilizing additive in cross-linked polyethylene pipe samples that were exposed to

https://doi.org/10.1021/acsapm.3c02209
ACS Appl. Polym. Mater. XXXX, XXX, XXX−XXX

recirculating hot water at different fixed temperatures for different aging times. Exposure of the inner pipe surface to hot water leads to hydrolysis of stabilizing additive molecules, creating small fragments that diffuse within the polyethylene matrix and leading to the outward radial propagation of hydrolysis. Our deep learning approach allowed us to identify the leading latent variable L1 associated with the hydrolysis process. At each aging time, we observed a sigmoidal radial profile L1 from which we defined the hydrolysis penetration depth δ as the midpoint of the best-fit sigmoidal curve. At each aging temperature, the dependence of δ on aging time t was well described by a $(t - t_0)^{1/2}$ dependence, corresponding to diffusion with an onset time t_0. Analysis of the temperature dependence of the diffusion coefficient D allowed us to determine the activation energy $E_a \sim 22\ k_B T$, indicating a high energy barrier to the diffusion process. By applying the principle of time−temperature superposition, we obtained a collapse of all of the data onto a master curve, which allowed us to determine that an increase in aging temperature of 10 °C produced a degree of hydrolysis that was equivalent to a decrease in the aging time by a factor of 1.8. Our results illustrate the advantage of the β-VAE analysis, providing a useful, interpretable representation of our very large data set and allowing us to achieve a detailed understanding of the stabilizing additive hydrolysis.

AUTHOR INFORMATION

Corresponding Author

John R. Dutcher − *Department of Physics, University of Guelph, Guelph, ON,, Canada N1G 2W1;* orcid.org/0000-0003-2594-5388; Phone: 519-824-4120; Email: dutcher@uoguelph.ca

Authors

Joseph D'Amico − *Department of Physics, University of Guelph, Guelph, ON,, Canada N1G 2W1*

Michael Grossutti − *Department of Physics, University of Guelph, Guelph, ON,, Canada N1G 2W1*

Complete contact information is available at: https://pubs.acs.org/10.1021/acsapm.3c02209

Notes

The authors declare no competing financial interest.

ACKNOWLEDGMENTS

The authors thank Peter Kazmaier and Ben Baylis for valuable discussions. J.R.D. is the recipient of a College of Engineering and Physical Sciences Research Chair in Novel Sustainable Nanomaterials. This work was supported by the Natural Sciences and Engineering Research Council of Canada [grant number CRDPJ-2018-531166].

REFERENCES

(1) Gijsman, P.; Dozeman, A. Comparison of the UV-degradation chemistry of unstabilized and HALS-stabilized polyethylene and polypropylene. *Polym. Degrad. Stab.* **1996**, *53*, 45−50.

(2) Grossutti, M.; Hiles, M.; D'Amico, J.; Wareham, W. C.; Morling, B.; Graham, S.; Dutcher, J. R. Quantifying Stabilizing Additive Hydrolysis and Kinetics Through Principal Component Analysis of Infrared Spectra of Cross-Linked Polyethylene Pipe. *Polym. Degrad. Stab.* **2022**, *200*, No. 109963.

(3) Wierer, M.; Buchberger, W.; Klampfl, C. W. Analysis and fate of the hindered amine light stabilizer Tinuvin 622 in polyester powder coatings using high performance liquid chromatography/time of flight mass spectrometry. *Polym. Test.* **2020**, *90*, No. 106677.

(4) Allen, N. S.; Edge, M. Perspectives on additives for polymers. Part 2. Aspects of photostabilization and role of fillers and pigments. *J. Vinyl Addit. Technol.* **2021**, *27*, 211−239.

(5) Maria, R. *Monitoring the degradation of PE pipes by IR-microscopy*. Ph. D. Thesis, Technical University of Darmstadt, 2014.

(6) Maria, R.; Rode, K.; Schuster, T.; Geertz, G.; Malz, F.; Sanoria, A.; Oehler, H.; Brüll, R.; Wenzel, M.; Engelsing, K.; Bastian, M.; Brendlé, E. Ageing study of different types of long-term pressure tested PE pipes by IR-microscopy. *Polymer* **2015**, *61*, 131−139.

(7) Scoponi, M.; Cimmino, S.; Kaci, M. Photo-stabilisation mechanism under natural weathering and accelerated photo-oxidative conditions of LDPE films for agricultural applications. *Polymer* **2000**, *41*, 7969−7980.

(8) Thörnblom, K.; Palmlöf, M.; Hjertberg, T. The extractability of phenolic antioxidants into water and organic solvents from polyethylene pipe materials − Part I. *Polym. Degrad. Stab.* **2011**, *96*, 1751−1760.

(9) Hiles, M.; Grossutti, M.; Dutcher, J. R. Classifying Formulations of Crosslinked Polyethylene Pipe By Applying Machine-Learning Concepts to Infrared Spectra. *J. Polym. Sci., Part B: Polym. Phys.* **2019**, *57* (18), 1255−1262.

(10) Whelton, A. J.; Dietrich, A. M.; Gallagher, D. L. Contaminant diffusion, solubility, and material property differences between HDPE and PEX potable water pipes. *J. Environ. Eng.* **2010**, *136*, 227−237.

(11) Bredács, M.; Frank, A.; Bastero, A.; Stolarz, A.; Pinter, G. Accelerated aging of polyethylene pipe grades in aqueous chlorine dioxide at constant concentration. *Polym. Degrad. Stab.* **2018**, *157*, 80−89.

(12) Hirabayashi, H.; Iguchi, A.; Yamada, K.; Nishimura, H.; Ikawa, K.; Honma, H. In *Evaluation of Durability and Structure of Peroxide Cross-linked Polyethylene Pipes with Several Stabilizers*, Annual Technical Conference - ANTEC, Conference Proceedings, 2013; pp 1494−1499.

(13) Lundbäck, M.; Strandberg, C.; Albertsson, A. C.; Hedenqvist, M. S.; Gedde, U. W. Loss of stability by migration and chemical reaction of Santonox R in branched polyethylene under anaerobic and aerobic conditions. *Polym. Degrad. Stab.* **2006**, *91*, 1071−1078.

(14) Whelton, A. J.; Dietrich, A. M.; Gallagher, D. L. Impact of chlorinated water exposure on contaminant transport and surface and bulk properties of high-density polyethylene and cross-linked polyethylene potable water pipes. *J. Environ. Eng.* **2011**, *137*, 559−568.

(15) Viebke, J.; Elble, E.; Ifwarson, M.; Gedde, U. W. Degradation of unstabilized medium-density polyethylene pipes in hot-water applications. *Polym. Eng. Sci.* **1994**, *34*, 1354−1361.

(16) Karlsson, K.; Smith, G. D.; Gedde, U. W. Molecular structure, morphology, and antioxidant consumption in medium density polyethylene pipes in hot-water applications. *Polym. Eng. Sci.* **1992**, *32*, 649−657.

(17) Stark, N. M.; Matuana, L. M. Surface chemistry and mechanical property changes of wood-flour/high-density-polyethylene composites after accelerated weathering. *J. Appl. Polym. Sci.* **2004**, *94*, 2263−2273.

(18) Pinheiro, L. A.; Chinelatto, M. A.; Canevarolo, S. V. The role of chain scission and chain branching in high density polyethylene during thermo-mechanical degradation. *Polym. Degrad. Stab.* **2004**, *86*, 445−453.

(19) Unruh, D.; Kolluru, V. S. C.; Baskaran, A.; Chen, Y.; Chan, M. K. Theory+AI/ML for microscopy and spectroscopy: Challenges and opportunities. *MRS Bull.* **2022**, *47*, 1024−1035.

(20) Yaman, M. Y.; Kalinin, S. V.; Guye, K. N.; Ginger, D. S.; Ziatdinov, M. Learning and Predicting Photonic Responses of Plasmonic Nanoparticle Assemblies via Dual Variational Autoencoders. *Small* **2023**, *19*, No. 2205893.

(21) Lu, S.; Jayaraman, A. Pair-Variational Autoencoders (PairVAE) for Linking and Cross-Reconstruction of Characterization Data from

Complementary Structural Characterization Techniques. *JACS Au* **2023**, *3*, 2510.
(22) Grossutti, M.; D'Amico, J.; Quintal, J.; MacFarlane, H.; Quirk, A.; Dutcher, J. R. Deep Learning and Infrared Spectroscopy: Representation Learning with a β-Variational Autoencoder. *J. Phys. Chem. Lett.* **2022**, *13* (25), 5787−5793.
(23) Grossutti, M.; D'Amico, J.; Quintal, J.; MacFarlane, H.; Wareham, W. C.; Quirk, A.; Dutcher, J. R. Deep generative modeling of infrared images provides signature of cracking in cross-linked polyethylene pipe. *ACS Appl. Mater. Interfaces* **2023**, *15*, 22532.
(24) Burgess, C. P.; Higgins, I.; Pal, A.; Matthey, L.; Watters, N.; Desjardins, G.; Lerchner, A. Understanding Disentangling in β-VAE, arXiv:1804.03599. arXiv.org e-Print archive. https://arxiv.org/abs/1804.03599 (accessed April 6, 2023).
(25) Higgins, I.; Matthey, L.; Pal, A.; Burgess, C.; Glorot, X.; Botvinick, M.; Mohammed, S.; Lerchner, A. β-VAE: Learning Basic Visual Concepts with a Constrained Variational Framework In *ICLR 2017*, 2016.
(26) Kingma, D. P.; Welling, M. Auto-encoding Variational Bayes. 2013, arXiv:1312.6114.
(27) Demšar, J.; Curk, T.; Erjavec, A.; Gorup, Č.; Hočevar, T.; Milutinovič, M.; Možina, M.; Polajnar, M.; Toplak, M.; Starič, A.; Štajdohar, M. Orange: data mining toolbox in Python. *J. Mach. Learn. Res.* **2013**, *14*, 2349−2353.
(28) https://www.tensorflow.org/tutorials/generative/autoencoder (accessed May 3, 2022).
(29) https://www.tensorflow.org/tutorials/generative/cvae (accessed May 3, 2022).
(30) https://keras.io/examples/generative/vae/ (accessed May 3, 2022).
(31) Abadi, M.; Agarwal, A.; Barham, P.; Brevdo, E.; Chen, Z.; Citro, C.; Corrado, G. S.; Davis, A.; Dean, J.; Devin, M.; Ghemawat, S.; Goodfellow, I.; Harp, A.; Irving, G.; Isard, M.; Jia, Y.; Jozefowicz, R.; Kaiser, L.; Kudlur, M.; Levenberg, J.; Mane, D.; Monga, R.; Moore, S.; Murray, D.; Olah, C.; Schuster, M.; Shlens, J.; Steiner, B.; Sutskever, I.; Talwar, K.; Tucker, P.; Vanhoucke, V.; Vasudevan, V.; Viegas, F.; Vinyals, O.; Warden, P.; Wattenberg, M.; Wicke, M.; Yu, Y.; Zheng, X. Tensorflow: Large-Scale Machine Learning on Heterogeneous Distributed Systems. arXiv:1603.04467. arXiv.org e-Print archive. https://arxiv.org/abs/1603.04467 (accessed April 6, 2023).
(32) Chollet, F. GitHub Repository, GitHub. 2015, https://github.com/fchollet/keras (accessed April 6, 2023).
(33) Kingma, D. P.; Ba, J. Adam: A Method for Stochastic Optimization. arXiv:1412.6980. arXiv.org e-Print archive. https://arxiv.org/abs/1412.6980 (accessed April 6, 2023).
(34) Rowe, R. K.; Abdelaal, F. B. Antioxidant Depletion in High-Density Polyethylene (HDPE) Geomembrane with Hindered Amine Light Stabilizers (HALS) in Low-pH Heap Leach Environment. *Can. Geotech. J.* **2016**, *53* (10), 1612−1627.
(35) Beißmann, S.; Stiftinger, M.; Grabmayer, K.; Wallner, G.; Nitsche, D.; Buchberger, W. Monitoring the Degradation of Stabilization Systems in Polypropylene During Accelerated Aging Tests by Liquid Chromatography Combined with Atmospheric Pressure Chemical Ionization Mass Spectrometry. *Polym. Degrad. Stab.* **2013**, *98* (9), 1655−1661.
(36) Bertoldo, M.; Ciardelli, F. Water Extraction and Degradation of a Sterically Hindered Phenolic Antioxidant in Polypropylene Films. *Polymer* **2004**, *45* (26), 8751−8759.
(37) Nagy, K.; Epacher, E.; Staniek, P.; Pukánszky, B. Hydrolytic Stability of Phenolic Antioxidants and its Effect on Their Performance in High-Density Polyethylene. *Polym. Degrad. Stab.* **2003**, *82* (2), 211−219.
(38) Tátraaljai, D.; Vámos, M.; Orbán-Mester, Á.; Staniek, P.; Földes, E.; Pukánszky, B. Performance of PE Pipes Under Extractive Conditions: Effect of the Additive Package and Processing. *Polym. Degrad. Stab.* **2014**, *99*, 196−203.
(39) Reingruber, E.; Buchberger, W. Analysis of Polyolefin Stabilizers and Their Degradation Products. *J. Sep. Sci.* **2010**, *33* (22), 3463−3475.
(40) Linde, E.; Giron, N. H.; Celina, M. C. Diffusion-limited hydrolysis in polymeric materials. *Polym. Degrad. Stab.* **2022**, *204*, No. 110095.
(41) Ferry, J. D. *Viscoelastic Properties of Polymers*, 3rd ed.; John Wiley & Sons: New York, 1980.
(42) Mehrer, H. *Diffusion in Solids: Fundamentals, Methods, Materials, Diffusion-Controlled Processes*, Springer Series in Solid-State Sciences, Springer-Verlag: Berlin, 2007; Vol. *155*., Chapter 8.

https://doi.org/10.1021/acsapm.3c02209
ACS Appl. Polym. Mater. XXXX, XXX, XXX−XXX